Estimating the atmospheric turbulence parameters from the wind velocity measured with a pulsed coherent CO_2 Doppler lidar

V.A. Banakh and A.V. Falits

Institute of Atmospheric Optics,
Siberian Branch of the Russian Academy of Sciences, Tomsk

We describe a technique for estimating the parameters of small-scale wind turbulence from the wind velocity measured with a pulsed CO_2 coherent Doppler lidar. The pulse length and the spatial resolution are taken to be several hundred meters. Numerical simulations of the lidar wind measurements in the turbulent atmosphere have been performed using real laser pulses emitted from a laser and recorded in the experiments with the WIND lidar system (Ch. Werner et al., Opt. Eng. **40**, 115–125 (2001)). The errors of the turbulent parameters estimates from lidar data have been calculated as well.

Introduction

At present, coherent Doppler lidars (CDL) find application in the investigations of wind fields in the atmosphere. The existing ground-based and airborne Doppler lidar systems[1–9] make it possible to measure the wind speed and direction with high spatial resolution. We present an overview of the techniques of estimating the wind velocity vector from the radial (along the propagation direction of a sounding beam) component of wind velocity measured with a CDL, as well as a comparative analysis of the accuracy of the techniques published in the literature.[10] The first measurement results on the wind turbulence parameters obtained using a CDL can be found in the literature,[22–24] the results of subsequent experiments on the study of turbulence and atmospheric air flows with the use of coherent Doppler lidars have also been published.[15,17,18,21, 25–30,35]

Analysis of the accuracy of the wind velocity measurements with coherent Doppler lidars and the potentialities of the reconstruction of parameters of wind turbulence from Doppler lidar data have been presented in Refs. 11–21, 37, and 38. Thus, in the papers by the researchers from the Institute of Atmospheric Optics, SB RAS and the Institute for Atmospheric Physics of the German Airspace Agency (see Refs. 11, 13, 15, and references therein) the problems due to the effect of spatial averaging over the volume sounded on the characteristics of the wind measured with a cw CO_2-laser-based lidar have been considered in detail. The effect of this averaging on the measured dissipation rate of the turbulence kinetic energy has also been taken into account. Frehlich with coauthors[17–20,31–33,37,38] have made an important contribution to the development of the

methods for estimating the wind velocity and parameters of small-scale atmospheric turbulence measured with a pulsed CDL systems operated at 2 μm wavelength. See also the bibliography in these papers. Statistics of wind velocity fluctuations, measured with a pulsed CDL at 2 μm and the possibilities of estimating the dissipation rate of turbulent energy and other turbulent parameters from these measurements have been discussed in Refs. 14 and 21.

Based on the above-mentioned papers, one can state that methical problems of estimating the wind velocity and parameters of small-scale turbulence from the wind velocity measured using a cw CO_2-laser-based and a pulsed CDL at 2 μm wavelength have been developed quite thoroughly. However, it is not the case with the pulsed CO_2-laser-based coherent Doppler lidars,[25,27–30] for which only in the Ref. 21 analysis was made of spatial spectra of wind velocity based on the numerical simulations. For this reason, many methical problems of using such lidars in the investigations of the atmospheric turbulence are still to be solved.

Thus, a long duration CO_2-laser pulse produces the scattering volume in the atmosphere that has too large extension along the direction of sounding. As a result, one cannot use the expressions for the statistical characteristics of wind fluctuations in determining the dissipation rate of the turbulence kinetic energy, since those are valid only in the inertial interval of the spectrum of turbulent fluctuations. It is just this feature of the pulsed CO_2-laser-based CDLs that make them disadvantageous as compared with the cw CO_2-laser-based CDLs and pulsed CDLs operated at 2 μm wavelength. The shape of a CO_2-laser pulse is much complicated, its

duration and amplitude fluctuate during the generation, that is an additional source of statistical uncertainty in estimating the turbulence parameters from the wind velocity measured with a pulsed CO_2-laser-based CDL.

In this paper we analyze, based on the results of numerical simulations, the possibility of estimating the dissipation rate of the turbulence kinetic energy and other turbulence parameters from data acquired with a pulsed CO_2-laser-based CDL. The simulations of the lidar wind measurements in the turbulent atmosphere have been performed using real laser pulses emitted from a laser and recorded in the experiments with the WIND lidar system.[8]

1. Numerical simulation of lidar returns and estimation of the Doppler wind velocity

In the case of a pulsed lidar, the signal component of the photodetector electric current j_s measured at a time t can be presented in the following form[14,31,32]:

$$j_s(t) = \mathrm{Re}\{y(t)\}, \qquad (1)$$

where

$$y(t) = 2\,\frac{e\eta_Q}{h\nu}\,\frac{K(R)}{R}\,P_L^{1/2}\sum_{l=1}^{n_s} P_T^{1/2}\,(t - 2z_l/c)\,\alpha_l \times$$

$$\times\, Q(\boldsymbol{\rho}_l)\exp\left[2jkz_l + 2\pi j\left(\Delta f - \frac{2}{\lambda}V_r(z_l)\right)t\right];$$

$$Q(\boldsymbol{\rho}_l) = R\lambda \int_{-\infty}^{\infty} d^2\rho\, W(\boldsymbol{\rho})\, A_L^*(\boldsymbol{\rho}) \int_{-\infty}^{\infty} d^2\rho'\, A_T(\boldsymbol{\rho}')W(\boldsymbol{\rho}')\times$$

$$\times\, G(\boldsymbol{\rho}_l,\,R;\,\boldsymbol{\rho}',\,0)\,G(\boldsymbol{\rho}_l,\,R;\,\boldsymbol{\rho},\,0);$$

n_s is the number of scattering particles in the atmosphere; $R = ct/2$ is the distance to the volume sounded; c is the speed of light; e is the electron charge; η_Q is the quantum efficiency of the photodetector; $h\nu$ is the photon energy;

$$K(R) = \exp\left\{\int_0^R dz'\alpha_a(z')\right\},$$

α_a is the extinction coefficient of the atmosphere;

$A_L(\boldsymbol{\rho}) = E_L(\boldsymbol{\rho})/P_L^{1/2}$ and $A_T(\boldsymbol{\rho}) = E_T(\boldsymbol{\rho},\,t)/P_T^{1/2}(t)$

are the normalized amplitudes of the light wave electric field;

$$P_T(t) = \int_{-\infty}^{\infty} d^2\rho\,|E_T(\boldsymbol{\rho},\,t)|^2 \text{ and } P_L = \int_{-\infty}^{\infty} d^2\rho\,|E_L(\boldsymbol{\rho})|^2$$

are the powers of sounding and reference beams, respectively;

$$U_p = \int_{-\infty}^{\infty} dt\, P_T(t)$$

is the sounding pulse energy; α_l is the scattering amplitude of the lth particle located at the point $\{z_l,\,\boldsymbol{\rho}_l\}$ (z is the propagation axis); $W(\boldsymbol{\rho})$ is the function of a pupil of the transmitting–receiving telescope; G is the Green's function, $k = 2\pi/\lambda$, λ is the wavelength of a sounding radiation; Δf is the intermediate frequency, and $V_r(z)$ is the radial component of the wind velocity at a distance z from the lidar.

From Eq. (1) we obtain[31] for the mean power of the signal component of the photocurrent $S = (1/2)\overline{y(t)y^*(t)}$ that

$$S = 2\,[e\eta_Q/(h\nu)]^2\,P_S P_L \eta_H, \qquad (2)$$

where $P_S = A_R\beta_\pi(R)K^2(R)cU_p/(2R^2)$ is the power of the return signal at incoherent detection;

$$A_R = \int_{-\infty}^{\infty} d^2\rho\, W^2(\boldsymbol{\rho})$$

is the area of the receiving-transmitting telescope;

$$\beta_\pi = \overline{\alpha_l^2}\,\rho_c$$

is the backscattering coefficient; ρ_c is the particle concentration;

$$\eta_H = A_R^{-1} \int_{-\infty}^{\infty} d^2\rho_l\,\overline{|Q(\boldsymbol{\rho}_l)|^2}$$

is the efficiency of heterodyning. Along with the signal component $y(t)$ the lidar receiving system also records the noise component of the photocurrent $n(t)$. In the case when the main source of noise is the shot noise occurring due to random events of the photoelectron production by the reference radiation (process described by the Poisson statistics), the mean noise power $N = \overline{|n|^2}$ is written as follows[34]:

$$N = 2\,e^2\eta_Q\,P_L B/(h\nu), \qquad (3)$$

where B is the transmission band of the receiver. Then the expression for the signal-to-noise ratio $SNR = S/N$ can be written in the form

$$SNR = \eta_Q\,\eta_H\,P_S/(h\nu B). \qquad (4)$$

The SNR quantity is the mean number of photoelectrons detected coherently for the time $\sim B^{-1}$ (Ref. 33).

From the sequence of the photocurrent samples acquired with a lidar we can pass to a complex signal

$$Z(mT_S) = \frac{1}{\sqrt{2}}\,y\,(t + mT_S) + n(mT_S), \qquad (5)$$

where $T_S = B^{-1}$ is the time of reading out the complex signal, $m = 0, 1, ..., M - 1$. The signal $Z(mT_S)$ satisfies the relations:

$$\overline{Z(mT_S)} = \overline{Z(mT_S)Z(lT_S)} = 0$$

and

$$\overline{Z(mT_S)Z^*(lT_S)} = SK_y(mT_S, lT_S) + N\delta_{ml},$$

where K_y is the correlation coefficient of the complex value of signal obtained by averaging the product $y(t + mT_S) y^*(t + lT_S)$ over all the random parameters of the medium, excluding the wind velocity, δ_{ml} is the Kronecker symbol ($\delta_{ml,m=l} = 1$, $\delta_{ml,m \neq l} = 0$).

Separating out the Doppler frequency f_D from the measured succession $Z(mT_S)$ can only be done within the limits of the Nyquist interval $[0, 1/T_S]$. Let us turn from $Z(mT_S)$ to $Z(mT_S) \exp[-2\pi j\Delta f mT_S]/\sqrt{N}$ and assume that $\Delta f = 1/(2T_S)$. Then taking the account of the Doppler ratio $V_D(R) = (\lambda/2)f_D$, we obtain that the estimate of the radial wind velocity $V_D(R)$ is within the interval $[-\lambda/(4T_S), \lambda/(4T_S)]$. After such a transition, we obtain, from Eqs. (1)–(5), for the correlation function of a complex signal

$$B_z(mT_S, lT_S) = \overline{Z(mT_S)Z^*(lT_S)}$$

the following formula:

$$B_z(mT_S, lT_S) = SNR \times$$

$$\times \frac{2}{cU_P} \int\limits_{-\infty}^{\infty} dz' P_T^{1/2}(mT_S - 2z'/c) P_T^{1/2}(lT_S - 2z'/c) \times$$

$$\times \exp\left[j \frac{4\pi}{\lambda}(l - m)T_S V_r(R + z')\right] + \delta_{ml}. \quad (6)$$

Simulation of signals has been performed as follows. The region in space occupied by a laser pulse $P_T(t)$ along the direction of propagation was subdivided into n_L layers, and the signal recorded at the time mT_S was presented by the sum of contributions from each layer and the noise

$$Z(mT_S) = \sqrt{\frac{SNR}{2\sum\limits_{k=0}^{n_L} P_T(\Delta pk)}} \sum\limits_{k=0}^{n_L} a(k + m) P_T^{1/2}(\Delta pk) \times$$

$$\times \exp\left\{-j \frac{4\pi}{\lambda} mT_S V_r[\Delta p(k + m)]\right\} + \frac{1}{\sqrt{2}} n_m, \quad (7)$$

where Δp is the layer thickness; $a(k)$ and n_m are the independent complex random numbers with the real and imaginary parts being distributed according to the Gaussian law with the zero mean and unit variance, V_r are the real random values of wind speed.

As a transmitted pulse $P_T(t)$ we took the sequence of records of real pulses of a CO_2-laser of the WIND[8] Doppler lidar. An example of such a pulse is given in Fig. 1.

From the set of real pulses the average pulse shape (Fig. 2) was found, which was used for testing the simulation algorithms and the calculation of the spatial structure function of the wind measured with lidar.
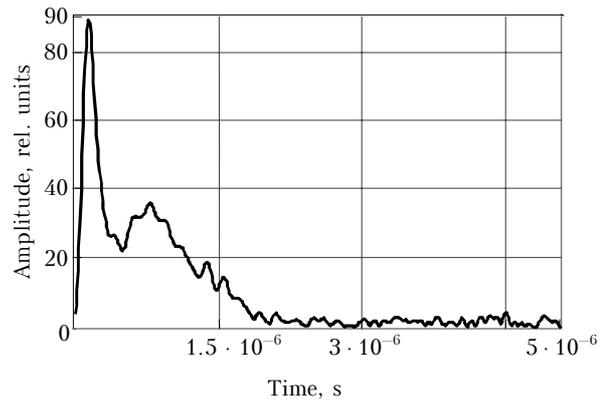

Fig. 1. An example of a CO_2 laser pulse used in lidar system WIND.
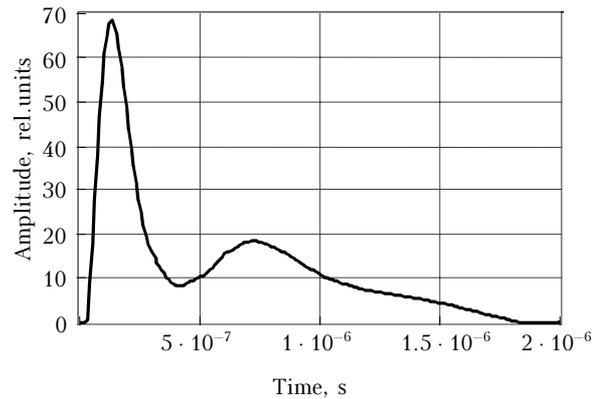

Fig. 2. Averaged laser pulse shape in WIND lidar obtained averaging over 5500 pulses.

The values of $V_r(\Delta pk)$ were simulated in the spectral range. The spectral components of the unit complex (Gaussian) white noise were multiplied by the coefficients satisfying the spectral density of turbulent fluctuations of wind velocity in the atmosphere:

$$S_r(\kappa) = \int\limits_{-\infty}^{\infty} dr \langle \widetilde{V}_r(R + r) \widetilde{V}_r(R) \rangle e^{-2\pi j\kappa r}, \quad (8)$$

where $\widetilde{V}_r = V_r - \langle V_r \rangle$, and then the inverse Fourier transform was used. As the spectrum $S_r(\kappa)$ the Karman model was used[36]:

$$S_r(\kappa) = 2\sigma_r^2 L_v/[1 + (8.43\kappa L_v)^2]^{5/6}, \quad (9)$$

V.A. Banakh and A.V. Falits

Vol. 17, No. 4 /April 2004/ Atmos. Oceanic Opt. 263

where L_v is the integral scale of correlation of wind velocity (outer scale of turbulence). At high frequencies $\kappa L_v > 1$ the spectral density $S_r(\kappa)$ must transform into the Kolmogorov–Obukhov spectrum[37]

$$S_r(\kappa) = 0.0375 C_k \varepsilon^{2/3} \kappa^{-5/3}, \qquad (10)$$

where $C_k \approx 2$ is the Kolmogorov constant; ε is the dissipation rate of the turbulence energy. Whence it follows that the parameters ε, σ_r^2, and L_v should relate through the ratio

$$\varepsilon = \frac{1.887}{C_k^{3/2}} \frac{\sigma_r^3}{L_v}. \qquad (11)$$

The simulation was made for $\lambda = 10.6$ μm, $T_S = 1 \cdot 10^{-8}$ s, $\Delta p = 1.5$ m, $n_L = 512$. From the obtained sequences of the signal $Z(mT_S)$ the radial velocity V_D was estimated from the argument of the correlation function (ACF-method)[38]:

$$V_D(R) = \lambda \arg [\hat{B}_z(T_S)]/(4\pi T_S), \qquad (12)$$

where

$$\hat{B}_z(T_S) = \frac{1}{M-1} \sum_{i=0}^{M-2} Z(iT_S) Z^*[(i+1)T_s]$$

is the unbiased estimate of the correlation function of the signal (6) with the time lag T_S.

2. Spatial structure function of the Doppler estimate of the wind speed

Spatial structure function of fluctuations of the Doppler estimate of the velocity $V_D(R)$

$$D(r) = \langle [\tilde{V}_D(R+r) - \tilde{V}_D(R)]^2 \rangle \qquad (13)$$

according to Ref. 14 can be presented in the form

$$D(r) = D_a(r) + D_e(r), \qquad (14)$$

where

$$\tilde{V}_D(R) = V_D(R) - \langle V_D(R) \rangle = \tilde{V}_a(R) + \tilde{V}_e(R);$$

$$D_a(r) = \langle [\tilde{V}_a(R+r) - \tilde{V}_a(R)]^2 \rangle$$

is the spatial structure function of the radial wind velocity averaged over the volume sounded;

$$D_e(r) = \langle [\tilde{V}_e(R+r) - \tilde{V}_e(R)]^2 \rangle$$

is the structure function of the estimate error of the Doppler velocity caused by fluctuations of the scattered wave and noises, $\tilde{V}_a$ and $\tilde{V}_e$ are independent.[37]

For the averaged over the volume sounded radial wind velocity we can obtain[14]:

$$V_a(R) = \frac{1}{U_p} \int_{-\infty}^{\infty} dt\, P_T(t) \frac{1}{\tau} \times$$

$$\times \int_{-\tau/2}^{\tau/2} dt'\, V_r \left[R + \frac{c}{2}(t+t') \right], \qquad (15)$$

where $\tau = MT_S$. From the latter we obtain that the structure function $D_a(r)$ is

$$D_a(r) = 2 \int_{-\infty}^{\infty} d\kappa S_r(\kappa)[1 - \exp(2\pi j\kappa r)] \times$$

$$\times \left(\frac{2}{\pi \kappa c \tau} \right)^2 \sin^2\left(\frac{\pi \kappa c \tau}{2} \right) \frac{1}{U_p^2} \int_{-\infty}^{\infty} dt_1 \int_{-\infty}^{\infty} dt_2\, P(t_1)P(t_2) \times$$

$$\times \exp[\pi j\kappa c(t_1 - t_2)]. \qquad (16)$$

Now we can present the structure function of the Doppler velocity estimate error in the following form

$$D_e(r) = 2[\sigma_e^2 - B_e(r)], \qquad (17)$$

where $B_e(r) = \langle [\tilde{V}_e(R+r)\,\tilde{V}_e(R)] \rangle$ and $\sigma_e^2 = B_e(0)$ are the correlation function and the variance of the Doppler velocity estimate error, respectively.

If we evaluate, following Refs. 14 and 38, the spatial structure function of the wind speed from the neighboring lidar returns:

$$D_p(r) = \langle [\tilde{V}_D^{(1)}(R+r) - \tilde{V}_D^{(2)}(R)] \rangle, \qquad (18)$$

where indices (1) and (2) refer to estimates of lidar return velocity of two neighboring transmissions of sounding pulses, then, with taking into account the independence of $V_a(r)$, $V_e^{(1)}(R)$ and $V_e^{(2)}(R)$, we obtain from Eq. (18) that

$$D_p(r) = 2\sigma_e^2 + D_a(r), \qquad (19)$$

where $2\sigma_e^2 = D_p(0)$.

We eliminate the variance of the estimate error from Eq. (19) and obtain the estimate of the structure function of radial wind velocity averaged over a volume sounded

$$\hat{D}_a(R) = D_p(R) - 2\sigma_e^2. \qquad (20)$$

Figure 3 shows the structure function of fluctuations of the radial component of the wind velocity and the structure function $D_a(R)$ calculated by the formula (16) ($M = 512$) and the estimate of $\hat{D}_a(R)$ (20) obtained from the simulation at the same parameters. Both the calculation and the simulation were made for the model of a sounding pulse $P_T(t)$ shown in Fig. 2. It is evident that both of these approaches yield identical results that evidences of the correctness of the simulation algorithm.
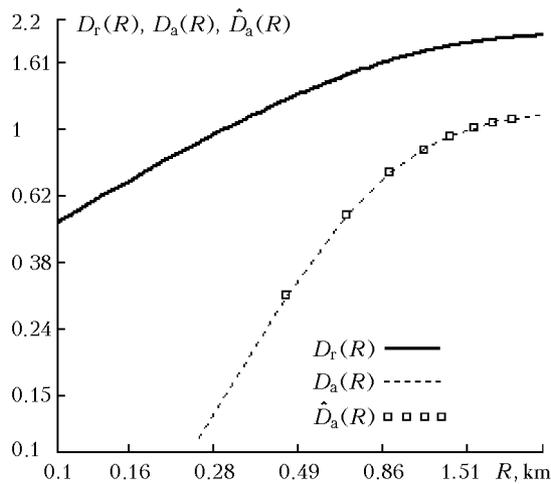
Fig. 3. Structure functions of the radial velocity D_r and radial velocity averaged over the volume sounded: D_a – calculation by the formula (16), $\hat{D}_a$ – simulation, $L_v = 500$ m, $\sigma_r^2 = 1$, $M = 512$.

3. The estimation of the wind turbulence parameters

For a cw CO_2-laser-based CDL and a pulsed CDL operated at $2\,\mu m$ wavelength the sounding range is, as a rule, not large and the effective longitudinal size Δz does not exceed the integral correlation scale of wind velocity. In this case, for estimating the parameters of wind turbulence and, in particular, the dissipation rate of the turbulent energy from wind velocity measured with lidar, it is possible to use the relations for statistical characteristics of wind velocity fluctuations in the atmosphere valid in the inertial interval of the spectrum of turbulent fluctuations. In this case for a pulsed CDL at $2\,\mu m$, when spacing $R \ll L_v$ is small, the spatial structure function $D_a(R) \sim \varepsilon^{2/3}$, and from lidar estimates of the spatial structure function we can obtain the solutions,[14] which enable us to determine the dissipation rate ε with an acceptable precision at a sufficiently large signal-to-noise ratio. Similar results for the cw CO_2-laser-based CDL can be found in the literature.[15]

The case with pulsed CO_2-laser-based CDL is quite different. In this case the spatial resolution of wind measurements ($MT_S c/2$) is hundreds of meters, and the scattering volume can compare in the length or even exceed the outer scale of turbulence. The effect of the outer scale will result in the fact that the spatial structure function of wind velocity measured with a pulsed CO_2-laser-based CDL, as a function of spacing R, will differ from the dependence $D_a(R)$, characteristic of the inertial interval.

Really, it follows from Fig. 4 that the region of dispersion, where the functions $D_a(R)$, calculated by Eq. (16) for the Kolmogorov (10) and Karman (9) spectra of the wind velocity fluctuations, coincide, is a negligible quantity.

The calculations were made for the time dependence of the pulse amplitude $P_T^{1/2}(t)$ given in Fig. 2 and different spatial resolution, i.e., at $MT_S c/2 = 300$ and 768 m. Thus, the determination of the dissipation rate of turbulent energy, as in the case with a 2-μm lidar,[14] from the estimate of spatial structure function of wind velocity at $R \ll L_v$ is impossible with a pulsed CO_2-laser-based CDL. Here it is necessary to take into account the effect of the outer scale of turbulence.
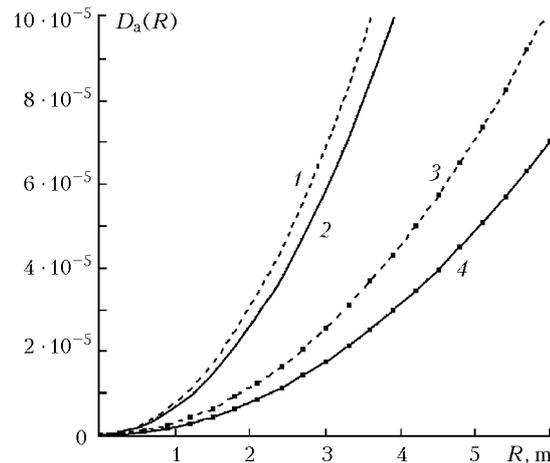

Fig. 4. Structure function $D_a(R)$ for the Kolmogorov and Karman spectra of turbulence calculated for measurements of wind velocity with different spatial resolution. (*1, 3*) Kolmogorov spectrum [Eq. (10)]; (*2, 4*) Karman spectrum [Eq. (9)]; $M = 200$ (*1, 2*); $M = 512$ (*3, 4*).

The dissipation rate ε can be found if we can use Eq. (11), but to determine the parameters σ_r^2 and L_v based on the spatial structure function of wind directly is also impossible in this case because, as it follows from expression (16), the value (9) depends on the product $\sigma_r^2 L_v$ and one and the same value of the structure function can correspond to different combinations of the values of these parameters. To avoid the ambiguity in choosing the parameters σ_r^2 and L_v the following procedure is proposed.

Using Eq. (16) we calculate the set of structure functions $D_a(L_{vi}; \sigma_r^2; R)$ (R varies from 0 to R_{max}) at different values of the outer scale L_{vi}. The value of the variance σ_r^2 in Eq. (16) may be arbitrary ($\sigma_r^2 = $ const). The choice of R_{max} is determined by the maximum separation, at which one can obtain in the experiment the estimation of the structure function (20). The value of R_{max} must be rather large, so that the structure function at R_{max} can be saturated, i.e., it is slightly depended on the separation. This makes it possible, by means of the normalization $D_a(L_{vi}; \sigma_r^2; R)$ to $D_a(L_{vi}; \sigma_r^2; R_{max})$, to get rid of the parameter σ_r^2:

$$\overline{D_a(L_{vi}; R)} = \frac{D_a(L_{vi}; \sigma_r^2; R)}{D_a(L_{vi}; \sigma_r^2; R_{max})}. \qquad (21)$$

Figure 5 shows an example of a set of normalized structure functions (21) calculated for different values of L_v
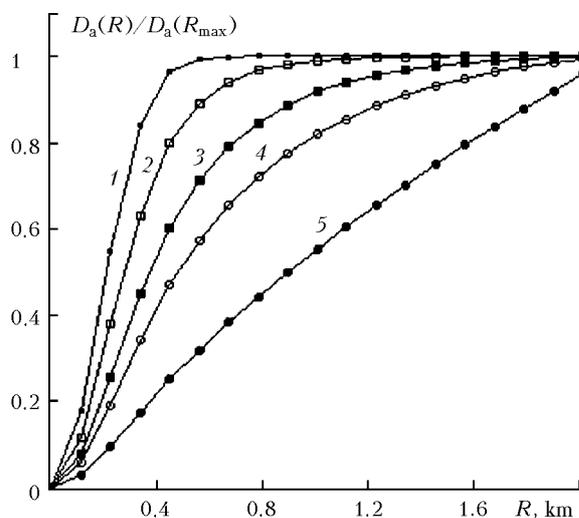

Fig. 5. Family of normalized structure functions calculated at different values of integral scale L_v for $M = 512$: $L_v = 50$ (*1*); 150 (*2*); 300 (*3*); 500 (*4*); and 1000 (*5*).

If an experimental estimation of the structure function $\hat{D}_a(R)$ (20) is normalized to $\hat{D}_a(R_{max})$: $\overline{\tilde{D}}_a(R) = \hat{D}_a(R)/\hat{D}_a(R_{max})$, we can use the method of parametric fitting and obtain the estimation of integral scale of the wind velocity fluctuations $\hat{L}_v$ by minimizing the functional

$$\sum_i \left[\overline{\hat{D}_a(R)} - \overline{D_a(L_{v_i}, R)} \right]^2. \qquad (22)$$

Using the estimation of the scale $\hat{L}_v$, one can find the variance estimate $\hat{\sigma}_r^2$:

$$\hat{\sigma}_r^2 = \frac{\hat{D}_a(R_{max})}{D_a(L_{v_i}, \sigma_r^2 = \text{const}, R_{max})}. \qquad (23)$$

According to the obtained estimations of the variance $\hat{\sigma}_r^2$ and the scale $\hat{L}_v$ the dissipation rates of turbulent energy $\hat{\varepsilon}$ are evaluated using the Eq. (1).

4. Results of numerical simulation

The numerical simulation of the signal was performed for a 10.6-μm pulsed Doppler lidar with the use of the WIND system in simulating the CO_2-laser pulses records (Fig. 1) at $T_S = 10^{-8}$ s and different signal-to-noise ratios. Separate random realizations of wind velocity were generated for the case of the Karman spectrum (9) at $\sigma_r = 1$ m/s and $L_v = 500$ m. The sample length was 4096 values of the velocity with the distance between readings

$\Delta p = 1.5$ m. In this case, according to Eq. (11), the dissipation rate of turbulent energy $\varepsilon = 1.33 \cdot 10^{-3}$ m^2/s^3. For an isolated pulse 2048 values were simulated, i.e., only one half of random realization of the velocity was used. The pulse repetition rate was set to be equal to 10 Hz, and it was assumed that during the next sounding event the wind realization is shifted by 1.5 m. Thus, one realization of wind V_r was used for simulating 1024 sounding events.

The values $M = 200$ and $M = 512$ were selected from the signal succession $Z(mT_S)$ that corresponded to the spatial resolution 300 and 768 m and the velocity V_D was estimated by the ACF method. For one realization of wind velocity 1849 estimates of V_D were obtained at $M = 512$. The total number of lidar estimates of the velocity, obtained from one wind realization, was 1024×1849 at $M = 200$ and 1024×1537 at $M = 512$. Overall we used 960 realizations of the wind velocity.

From that large array of data on V_D the structure function $\hat{D}_a(R)$ was estimated by varying the number of "shots" from 600 to 18000. For the pulse repetition frequency of 10 Hz this corresponds to the time from 1 to 30 min.

Then using the algorithm of Eqs. (21)–(23) and (11) the estimates of $\hat{L}_v$, $\hat{\sigma}_r^2$, $\hat{\varepsilon}$ with the values of these parameters obtained at simulation of the turbulent wind field, we calculated the dependences of the relative errors of estimation of the turbulence parameters on the time of averaging T. The results obtained are given in Fig. 6. It is evident from Fig. 6 that for the signal-to-noise ratios ≥ 2 the relative error of the reconstruction of the parameters σ_r^2 and ε from lidar data is in the range $< 50\%$ already at 5 minutes averaging that is appropriate for geophysical measurements. The situation is different with the integral scale of the velocity correlation. Here the relative error at a 5 min averaging is 70–80% and decreases slightly with the increase of averaging time.

Conclusion

We have described the technique of estimating the parameters of small-scale wind turbulence from the data of wind measurements performed by means of a pulsed CO_2-laser—based CDL, for which the pulse length and the spatial resolution are several hundreds of meters. The numerical simulations performed show that for a sufficiently large data samples and 300-m spatial resolution of wind measurements the estimation error in the dissipation rate of turbulent energy does not exceed 30%; the error in the variance of the velocity fluctuations is 10%, and in the integral scale of correlation it is 70%, at the signal-to-noise ratio ≥ 2. The relative error of evaluating the dissipation rate increases with the decreasing spatial resolution of lidar returns sampling and at the spatial resolution of 768 m it is 65–70%, at a half-hourly averaging.
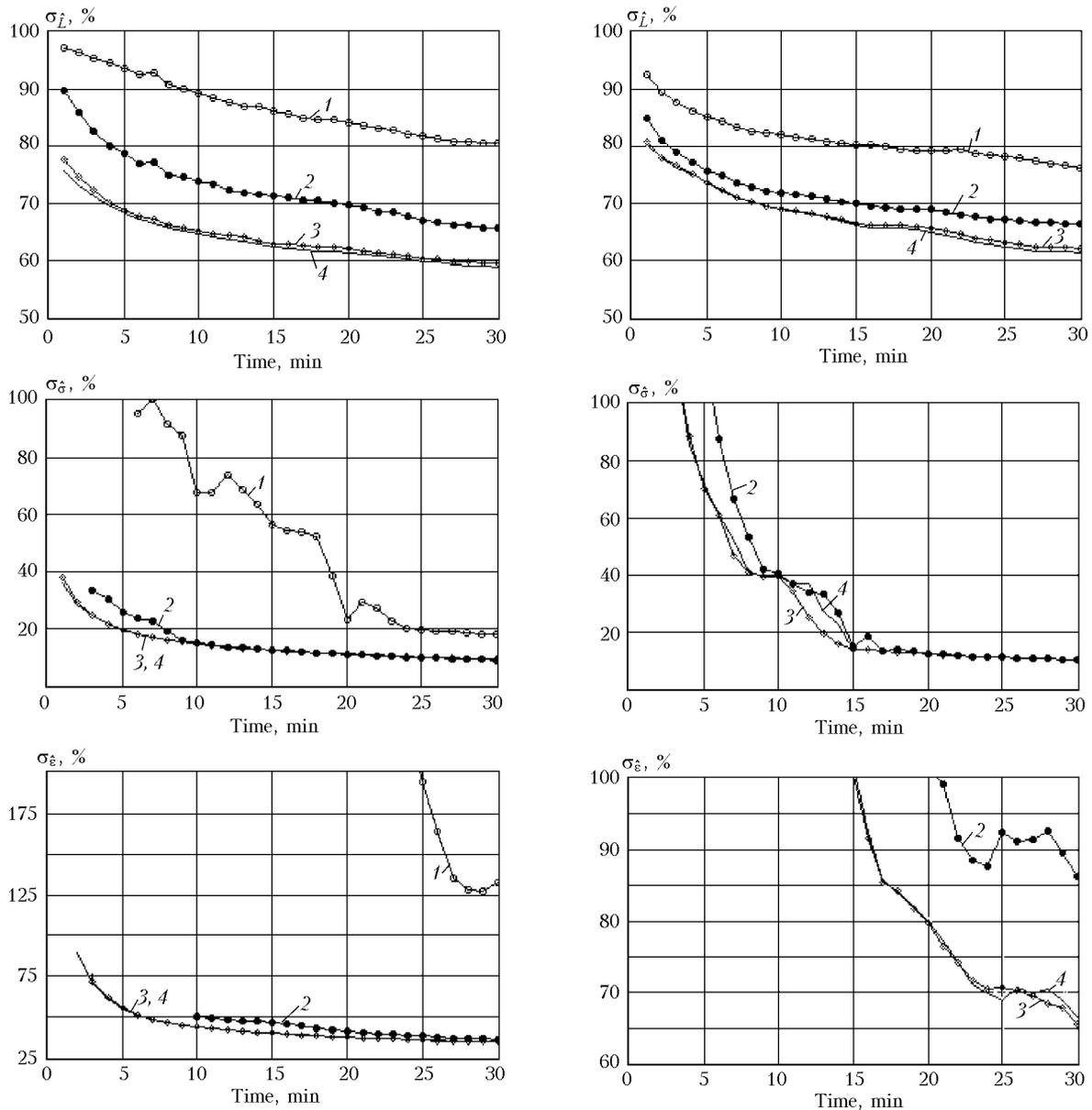
Fig. 6. Relative error of measurement of turbulence parameters: $M = 200$, spatial resolution is 300 m (a); $M = 512$, spatial resolution is 768 m (b); SNR = 1 (1); 2 (2); 5 (3); and 10 (4).

Acknowledgments

References

1. S.W. Henderson, C.P. Hale, J.R. Magee, M.J. Kavaya and A.V. Huffaker, Opt. Lett. **16**, 773−775 (1991).
2. S.W. Henderson, P.J.M. Suni, C.P. Hale, S.M. Hannon, J.R. Magee, D.L. Bruns, and E.H. Yuen, IEEE Trans. Geosci. Remote Sens. **31**, 4−15 (1993).
3. S.F. Clifford, J.C. Kaimal, R.J. Lataitis, and R.G. Strauch, Proc. IEEE **82**, 313−355 (1994).
4. M.R. Huffaker and R.-M. Hardesty, Proc. IEEE **84**, 181−204 (1996).

5. J.M. Vangham, O. Steinvall, C. Werner, and P.H. Flamant, Proc. IEEE **84**, 205−226 (1996).
6. J.M. Wilczak, E.E. Gossard, W.D. Neff, and W.I. Ebarhard, Boundary Layer Meteorol. **78**, 321−349 (1996).
7. J. Rothermel, C. Kessinger, and D.L. Davis, J. Atmos. Oceanic Technol. **2**, 138−147 (1985).
8. Ch. Werner, P.H. Flamant, O. Reitebuch, F. Kopp, J. Streicher, S. Rahm, E. Nagel, M. Klier, H. Herrmann, C. Loth, P. Delville, Ph. Drobinski, B. Romand, Ch. Boitel, D. Oh, M. Lopez, M. Meisonnier, D. Bruneau, and A. Dabas, Opt. Eng. **40**, 115−125 (2001).
9. O. Reitebuch, Ch. Werner, I. Leike, P. Delville, P. Flamant, A. Cress, and D. Engelbart, J. Atmos. Ocean. Technol. **18**, 1331−1344 (2001).
10. I.N. Smalikho, J. Atmos. Ocean. Technol. **20**, 276−291 (2003).

V.A. Banakh and A.V. Falits

Vol. 17, No. 4 /April 2004/ Atmos. Oceanic Opt. 267

11. V.M. Gordienko, A.A. Kormakov, L.A. Kosovsky, N.N. Kurochkin, G.A. Pogosov, A.V. Priezzhev and Y.Y. Putivskii, Opt. Eng. **33**, 3206−3213 (1994).

12. V.A. Banakh, I.N. Smalikho, F. Kopp, and Ch. Werner, Appl. Opt. **34**, No. 12, 2055−2067 (1995).

13. V.A. Banakh and I.N. Smalikho, Atmos. Oceanic Opt. **10**, Nos. 4−5, 295−302 (1997).

14. V.A. Banakh, I.N. Smalikho, Atmos. Oceanic Opt. **10**, No. 12, 957−965 (1997).

15. V.A. Banakh, F. Kopp, Ch. Werner, and I.N. Smalikho, J. Atmos. Oceanic Technol. **16**, No. 8, 1044−1061 (1999).

16. V.A. Banakh, Ch. Werner, V. Vergen, A. Kress, N.P. Krivolutskii, I. Leike, I.N. Smalikho, and I. Schtreicher, Atmos. Oceanic Opt. **14**, No. 10, 848−855 (2001).

17. R. Frehlich, S. Hannon, and S. Henderson, Appl. Opt. **36**, 3491−3499 (1997).

18. R. Frehlich, S. Hannon, and S. Henderson, Boundary Layer Meteorol. **86**, 233−256 (1998).

19. R. Frehlich and I. Cornman, J. Atmos. Oceanic Technol. **19**, 355−366 (2002).

20. R. Frehlich, in: *Proc. of 12th Coherent Laser Radar Conference* (Bar Harbor Maine, US, 2003), pp. 139−142

21. Ph. Drobinskii, A. Dabas, and P.H. Flamant, J. Appl. Meteorol. **39**, 2434−2451 (2000).

22. G.M. Ancellet, R.T. Menzies, and W.B. Grant, J. Atmos. Oceanic Technol. **6**, 50−58 (1989).

23. W.L. Eberhard, R.E. Cupp, and K.R. Healy, J. Atmos. Oceanic Technol. **6**, 809−819 (1989).

24. T. Gal-Chen, M. Xu, and W.L. Eberhard, J. Geophys. Res. **97**, 18409−18423 (1992).

25. K.E. Bozier and C.G. Collier, in: *Proc. of 11th Coherent Laser Radar Conference* (Malvern, Worcestershire, U.K., 2001), pp. 206−209.

26. P. Drobinskii et al., in: *Reviewed and Revised Papers Presented at the Twenty-First International Laser Radar Conference (ILRC21)* (Quebec, Canada, 2002), ed. by L.R. Bissonnette, G. Roy, and G. Vallee, pp. 853−856.

27. O. Reitebuch, H. Volkert, Ch. Werner, A. Dabas, P. Delville, Ph. Drobinski, P.H. Flamant, and E. Richard, Quart. J. Roy. Meteorol. Soc. **129**, 715−728 (2003).

28. S.M. Hannon, P. Gatt, S.W. Henderson, and R.M. Huffaker, in: *Proc. of 12th Coherent Laser Radar Conference* (Bar Harbor Maine, US., 2003), pp. 86−89.

29. O. Reitebuch, Ch. Werner, A. Dabas, P. Delville, Ph. Drobinski, and L. Gantner, in: *Proc. of 12th Coherent Laser Radar Conference* (Bar Harbor Maine, US, 2003), pp. 102−105.

30. V. Banakh, Ch. Werner, I. Streicher, O. Reitebuch, E. Nagel, T. Schneiderhan, T. Konig, S. Lehner, A. Dabas, and P. Delville, in: *Proc. of 12th Coherent Laser Radar Conference* (Bar Harbor Maine, US, 2003), pp. 191−196.

31. R. Frehlich, and M.J. Kavaya, Appl. Opt. **30**, No. 36, 5325−5352 (1991).

32. R. Frehlich, Appl. Opt. **33**, No. 27, 6472−6481 (1994).

33. R. Frehlich and M.I. Yadlowsky, J. Atmos. Oceanic Technol. **11**, 1217−1230 (1994).

34. A. Van der Ziel, *Noise in Measurement* (Wiley, New York, 1976).

35. R.M. Hardesty, W.A. Brewer, S.P. Sandberg, C.I. Senff, B.I. McCarty, A.M. Weickmann, L. Ehert, A. Fix, G. Poberaj, M. Wirth, and C. Kiemle, in: *Proc. of 12th Coherent Laser Radar Conference* (Bar Harbor Maine, US, 2003), pp. 182−185.

36. N.K. Vinnichenko, N.Z. Pinus, S.M. Shmeter, and G.N. Shur, *Turbulence in the Free Atmosphere* (Gidrometeoizdat, Leningrad, 1976), 287 pp.

37. R. Frehlich, S.M. Hannon, and S.W. Henderson, J. Atmos. Oceanic Technol. **11**, No. 6, 1517−1528 (1994).

38. R. Frehlich, J. Atmos. Oceanic Technol. **14**, 54−75 (1997).